Seismic Analysis and Experimental Validation for the Column-supported Concrete Group Silos Structure

qikeng xu (xuqikeng@haut.edu.cn)
Henan University of Technology https://orcid.org/0000-0002-8060-9507
Yonggang Ding
Henan University of Technology
Jia Chen
Henan University of Technology
Qiang Liu
Henan University of Technology

Research Article

Keywords: Column-supported concrete group silos structure, Coupling effect, Simplified calculation method, Base shear distribution coefficient

Posted Date: April 19th, 2022

DOI: https://doi.org/10.21203/rs.3.rs-1561780/v1

Seismic Analysis and Experimental Validation for the Column-supported Concrete Group Silos Structure

Yonggang Ding[1,2], Qikeng Xu [*1,2], Jia Chen[1], Qiang Liu[1]

[1.] School of Civil Engineering and Architecture, Henan University of Technology, Zhengzhou, 450001, PR China

[2.] Henan Key Laboratory of Grain and Oil Storage Facility & Safety, HAUT, Zhengzhou, 450001, PR China

Abstract: At present, codes of practice rely on the single-silo seismic calculation to assess the seismic performance of the column-supported concrete group silos structure (CSCGSS). It is unreasonable proved by the work given in this paper. To more accurately calculate the earthquake action of a CSCGSS, the dynamic model of the overall structure considering the effect of dynamical coupling between different single silo in group silos is established for the first time. More in detail, based on linear elastic theory and multiple-degrees of freedom system motion, the model is used to analyze the base shear of CSCGSS with different storage mass conditions. Moreover, the computational model and the finite model are validated as reasonable through a shaking table test. Finally, the traditional vibration displacement superposition method for the single silo is updated to calculate the seismic action of the CSCGSS by defining the base shear force distribution coefficient to reflect the dynamical coupling effect in group silos. The results show that the frequency of CSCGSS decreases with the increasing quality of the stored material. Compared with the independent single silo, the base shear of group silos is uniformly distributed to different single silos under earthquake, but its value is not a simple superposition composed of the single silo. The base shear distribution coefficient acquired in the case of the empty, half, and full condition is tabulated and so a simplified calculation method is provided for engineers with a simple and accurate tool to estimate the seismic capacity of CSCGSS.

Keywords: Column-supported concrete group silos structure; Coupling effect; Simplified calculation method; Base shear distribution coefficient.

1. Introduction

As an upright container, silos are often used to store bulk materials, such as cereals, coal, and cement. With the increase in granary construction, some column-supported concrete group silos structures composed of single silo and row silos are gradually developed into large-diameter combined structure system, including the Dalian Beiliang Port group-silos composed of 128 single ones in China. As a special structure, the column-supported

* Corresponding author. E-mail: xuqikeng@haut.edu.cn

concrete group silos structure (CSCGSS) with large capacity, small area, easy mechanization, automatic operation, and low circulation cost can improve the efficiency of mechanization for grain storage. In view of this, the CSCGSS has been widely used in the storage structure.

However, Chinese codes of practice rely on the single-silo seismic experience formulas and construction requirement criteria to assess the seismic capacity of CSCGSS. The dynamical coupling effect of different single silos in CSCGSS is ignored, especially for the group silo design under the earthquake action. To ensure the safety of such grain storage structure and regular operation of the urban lifeline project after an earthquake, it is necessary to find a calculation method to assess the seismic capacity of CSCGSS under different storage mass conditions, develop design, and construction recommendations for such structures.

To date, much dynamic response research on group silos structure with different structural forms and discharge processes have been performed by experts. Nielsen (1998) revealed several phenomena contributing to pressure variations during flow discharge and found a most dangerous phenomenon that silo pressures are quite unsymmetrical even in symmetrical silos. Mahmoud and Kamel (2020) studied the failure mechanism of toluene storage tanks with different capacities. Kirtas et al. (2020) explored the modal response of steel cylindrical tank and the associated prevailing frequencies in the horizontal impulsive mode of vibration, considering soil-structure interaction. Results highlight a dominant rigid-body mode with the flexibly-supported system's lateral fundamental period. Pascot et al. (2020) performed experimental measurements and discrete element simulations (DEM) in a 2D dimensional silo to explore the influence of mechanical vibrations on silo discharges of granular matter. Hashemi et al. (2022) studied the dynamic behavior of concrete rectangular tanks subjected to motions caused by an earthquake considering the effects of soil-structure-fluid interaction. The results show that dynamic soil-tank interaction under an earthquake can cause a profound effect on the amplification of hydrodynamic forces and moments exerted on the tank structure.

Theoretical researches and experimental investigations for steel silos have been further carried out. Bayraktar et al. (2010) studied the seismic performance of cylindrical steel storage tanks by updating parameters related to FEM model. Based on Galerkin’s weighted residual technique, Chowdhury and Singh (2013) proposed a method to estimate the dynamic pressures induced on the rectangular bunker wall due to earthquake force, with the three sides fixed and one side hinged boundary conditions adopted. Durmuş and Livaoglu (2015) proposed a simplified finite model, analyzed influencing factors for displacement and base shear forces decline, taking into account the effects between the foundation of the silo and the soil. Chen et al. (2018) analyzed the effect of temperature patterns on silo wall by FEM and modified the nonlinearity of soil and reinforced concrete base on the D-P elastic-plastic criterion. Silvestri et al. (2022) conducted some shaking table tests on a full-scale flat-bottom steel

silo filled with soft wheat and found that the dynamic overpressures appear to increase with depth (differently from the EN1998-4 expectations) and to be proportional to the acceleration. Hasan et al. (2022) conducted an assessment to evaluate the crack and remaining strength of the cement plant blending silo structure and proposed the combination of epoxy resin injection and carbon fiber reinforced polymer (CFRP) wrapping to retrofit the structure.

In China, the seismic research of reinforced concrete silos receiving much concern has always been a concern of engineers. Zhang (2010) studied the group silos earthquake response and damage laws by the shaking table test of cylinder-supported by group silos models. Gong et al. (2014) obtained the theoretical solution of the vibration frequency and pattern of the RC column-supported vertical cylinder group silos by Hamiltonian principle. Guo et al. (2016) used the hypoplastic constitutive model to assess the seismic vulnerability of a RC silo located in Zhoushan, China. Xu (2019) studied the group silos earthquake response and damage laws by the shaking table test of column-supported by group silos models (2×3 combination) in the state key laboratory of disaster reduction in Tongji University civil engineering. Li et al. (2021) performed some experiments on RC vertical cylinder group silos structures to study the dynamic characteristics and seismic response of group silos structures.

Based on numerous studies results, some defects in the European specification are pointed out in the research of guiding engineering practice. Sezen et al. (2008) found that the axial and lateral strength of the columns supporting the two nearly full tanks were not sufficient to resist the demand imposed during the earthquake, according to the dynamic analysis results from a simplified three-mass model and a finite element model. Djelloul, and Mohammed (2018) investigated the reliability of the European guidelines employed for designing the steel silos subjected to seismic excitations and discussed the stress state and the profile of dynamic material pressure inadequate. Djelloul and Mohammed (2018) introduced the defects for curves of steel silo stress states and dynamic material pressure calculated by European norms. Gandia et al. (2021) tested six different types of silo geometry (slenderness and hopper angle) by filling the silo to the different heights of interest and observed a static phase (10 min) followed by complete discharge. Results proved that the lateral pressure ratio and the maximum frictional pressures are higher than those given in the Eurocode. Silvestri et al. (2022) conducted some shaking table tests on a full-scale flat-bottom steel silo filled with soft wheat and found that the dynamic overpressures appear to increase with depth (differently from the EN1998-4 expectations), and to be proportional to the acceleration.

In summary, many studies on the single silo dynamic behavior have been conducted by researchers, but few covered the seismic design method of group silos in the case of dynamic coupling interaction of single one in

different positions for group silos in CSCGSS. In this paper, based on linear elastic theory, the dynamic model of CSCGSS overall structure was established. The numerical investigation and shaking table tests of CSCGSS were carried out to analyze the base shear force. A dynamic simplified calculation method of CSCGSS was proposed for seismic calculation of such structures by adopting shear distribution coefficients. The simplified calculation procedure is presented to provide engineers with a simple and accurate tool to estimate the seismic response of CSCGSS.

2. Analytical Method

2.1 Basic Assumptions

It is assumed that there is no torsional effect in group silos. The deformation of the structure follows the elasticity. So, a multiple degrees of freedom system was established in this paper according to Rajasekaran (2009). The following hypotheses should be satisfied:

1) The total mass of the column-supported concrete group silos structure (CSCGSS) and the granular material is simplified to several mass points along with the height of the silo, such as m_1, m_2, …, and m_i, m_n;

2) The silo body between the mass points is regarded as an equal-sectional space pole unit with only provided stiffness;

3) The effect of group silos axial force on lateral displacement is ignored.

Further, the simplified mechanical model is shown in Fig. 1.

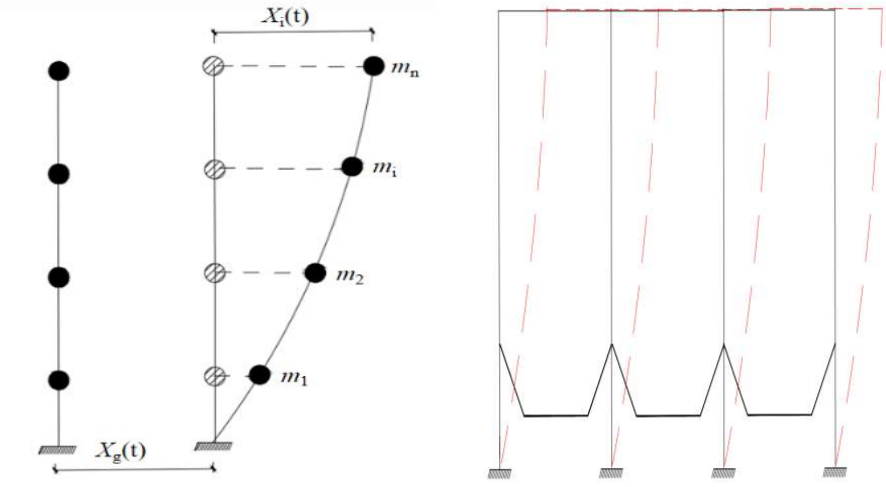

Fig. 1 The simplified mechanical model under horizontal earthquake action

2.2 Structural Dynamic Equation

Based on Darren Bell principle, the motion equations of equilibrium is formed by the horizontal inertial forces, elastic recovery forces and damping forces at the mass point *i*. The dynamic equation of CSCGSS under earthquake can be built by the Eq. (1):

$$[M]\{\ddot{x}(t)\}+[C]\{\dot{x}(t)\}+[K]\{x(t)\}=-[M]\{I\}\ddot{x}_{g}(t) \tag{1}$$

where, [M] is the CSCGSS mass matrix; [K] is structure stiffness matrix; [C] is structure damping matrix, and it can be expressed as [C]= α[M]+β[K]. {$x(t)$} is the displacement column vector of the mass points for CSCGSS relative to the ground, $\{\dot{x}(t)\}$ is the velocity column vector and $\{\ddot{x}(t)\}$ is the acceleration column vector. {I} is the unit column vector. $\{\ddot{x}_{g}(t)\}$ is the ground motion acceleration.

The characteristic equations of the Eq. (1) can be obtained, as shown in Eq. (2):

$$([K]-\omega^{2}[M])\{\varphi\}=\{0\} \tag{2}$$

where, {ϕ} is the amplitude of the free vibration of the CSCGSS mass point.

The dynamical eigenvalue equation for the CSCGSS is expressed as Eq. (3).

$$\left|[K]-\omega^{2}[M]\right|=0 \tag{3}$$

From Eq. (3), the self-vibration circle frequencies ω_i of the CSCGSS can be calculated. Taking the $\omega_1^2,\omega_2^2,\cdots,\omega_n^2$ into the Eq. (2), the vibration of the CSCGSS at each mass point can be obtained, as shown in Eq. (4).

$$\{\phi\}_j=\left[\phi_{j1},\phi_{j2},\cdots,\phi_{ji},\cdots,\phi_{jn}\right]^{T} \tag{4}$$

where, ϕ_{ji} is the relative horizontal displacement at the i-th particle and the j-th mode of vibration.

Since the vibration type satisfies the orthogonality principle, the displacement reaction of the CSCGSS at the i-th mass point in the vibration process can be expressed in Eq. (5).

$$\{x(t)\}=[\phi]\{\eta(t)\}=\sum_{j=1}^{n}\eta_j(t)\phi_{ji} \tag{5}$$

Where, $\eta_j(t)$ is the generalized coordinate of the j-th mode of vibration.

According to the response spectrum method in Gupta and Hall (2017), the seismic action of the CSCGSS can be shown in Eq. (6)

$$F_{ji}=\alpha_j\gamma_j\varphi_{ji}G_i\left(i=1,2,\cdots,n;\ j=1,2,\cdots,m\right) \tag{6}$$

Where, α_j is the seismic influence coefficient of the j-th mode of the self-vibration period. G_i is the gravity of the i-th mass point. γ_j is the participation coefficient of the j-th mode of vibration for the CSCGSS and it can be obtained in Eq. (7).

$$\gamma_j = \frac{\{\varphi\}_j^T [M][I]}{\{\varphi\}_j^T [M]\{\varphi\}_j} = \frac{\sum_{i=1}^{n} M_i \varphi_{ji}}{\sum_{i=1}^{n} M_i \varphi_{ji}^2} \quad (7)$$

3. Test Investigation

The unidirectional horizontal-displacement earthquake shaking table at Henan University of Technology was used. It was a servo-hydraulic system and the specific parameters were as follows: It was a servo-hydraulic system and the specific parameters were as follows: the table size was 3.00m×3.00m; the displacement limit ±100 mm; the maximum load 50t; and the frequency ranged from 0.1Hz to 50Hz. The scaled test model was based on a prototype column-supported reinforced concrete group silos with a height of 40.0m in shanghai Waigaoqiao. The support column height is 8.0m. The silo wall thickness is 0.22m. The whole test model was fixed on the shaking Table, and the column-supported was designed to be anchored on the bottom plate.

According to the proportion of shaking table and prototype group silos, the geometric similarity ratio was set as 25, from which the geometry size of the group silos was determined. Considering the reinforced concrete group silos test model with large stiffness and small deformation designed according to the similarity ratio, the group silos were made by PMMA. In addition, the study on the visualization of the 3-dimensional trajectory of particles was designed according to the PMMA model. PMMA model can be used repeatedly. The properties of the experimental model are shown in Tab. 1.

Tab. 1 Materials Parameters (Test)

Materials	Density ρ/(kg·m^{-3})	Elastic modulus E/MPa	Cohesion c/kPa	Friction angle φ/(◦)	Poisson's ratio v	Friction coefficient μ
PMMA	1180	3050	90	/	0.3	0.25
Machine-made sand	1340	0.2	/	35	/	0.45

In the test, the mechanical sand was selected to replace the particle in the silos. After the screening test, the sand size was determined as 1.18~2.36mm. In the case of half and full condition, the particle mass in the silos was added to the silo wall in the form of 4 lumped mass. According to the underartificial model design, the equivalent mass density similar proportional coefficient was obtained. (S_ρ=2.0) Based on similarity relationship principle, the test model's similarity coefficient choired can be determined by Zhou and Lv (2016). The seismic waves with acceleration peak of 0.0625g, 0.125g, 0.159g, 0.25g, and 0.281g were applied to the test models along the X direction of the shaking table. The El-Centro, Tangshan, and artificial waves were selected for the test. The shaking table used in

this study vibrates in the east-west direction. The measuring points of the model group silo and sensors are shown in Fig. 2. The independent single silo shaking table test completed by the research group, in Xu (2019), was treated as the comparison group.

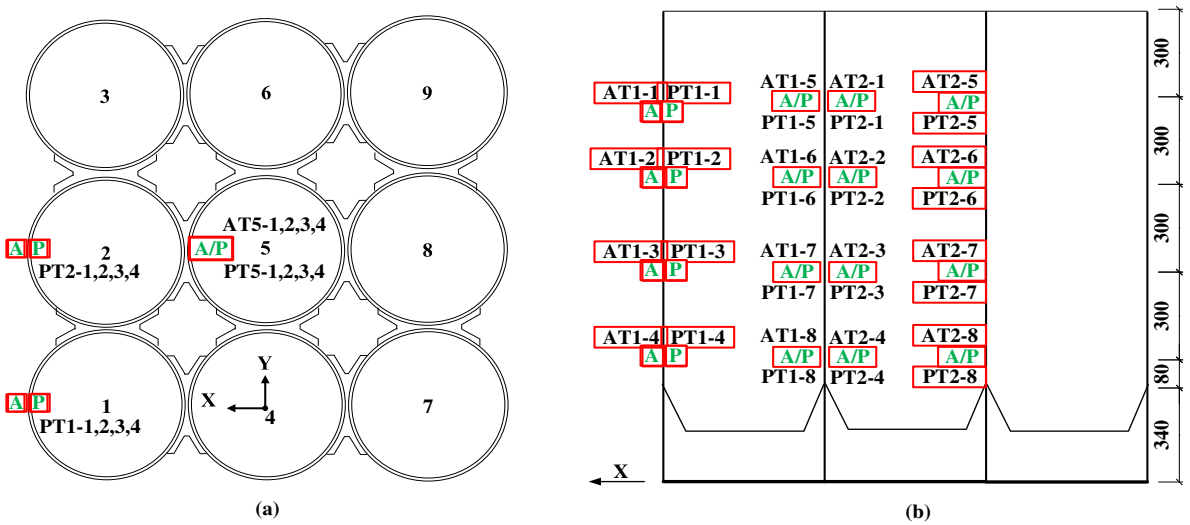

(c)

(d)

Fig. 2 Test Model: a) Measuring points setting of transducers layout; b) Measuring points setting of transducers vertical section; c) group silos with the empty condition; d) group silos with full condition

4. Numerical Investigation

In the ABAQUS model, the structure and storage materials element are C3D8R. An 8-node solid element is adopted for the bottom column-supported in the finite element analysis system. Each node of the solid element has three translation freedom degrees and can withstand various loads. To avoid the penetration of particle block into

wall, the contact was defined as limited sliding. The friction was tangential, hard contact was set to normal, and the friction coefficient between particle block and silo wall was 0.45. The boundary condition with fixed constraints was applied at the bottom of the group silos structure. Considering the subsequent related studies, especially for the grain movement problem, PMMA was applied to the finite element model to meet the visualization requirements trajectory of particles. The material parameters of the column-supported concrete group silos structure (CSCGSS) are shown in Tab. 2. The schematic diagram of the structural and storage materials element meshing is shown in Fig. 3.

Tab. 2 Materials Parameters (FEM)

Materials category	Density ρ/(kg·m^{-3})	Friction coefficient μ	Internal friction angle φ/(◦)	Elastic modulus E/MPa	Tensile strength σ_t (MPa)	Compressive strength σ_c (MPa)
PMMA	1180	/	/	3000	106.8	34.5
Sand	1340	0.45	35	0.2	/	/

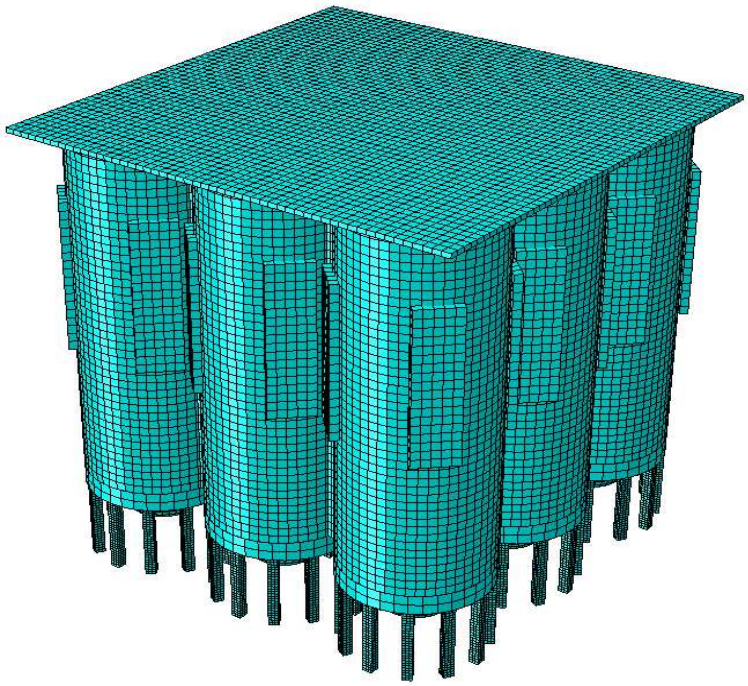

Fig. 3 ABAQUS Model of CSCGSS

The vibration modal analysis is an essential process during the seismic performance analysis. The preceding three mode shapes of group silos structure and single silo with empty, half, and full conditions are calculated through modal analysis in the ABAQUS. The modal results with different conditions are shown in Tab. 3.

Tab. 3 Modal analysis

Storage condition	Empty	Half	Full
Group silos mode shapes	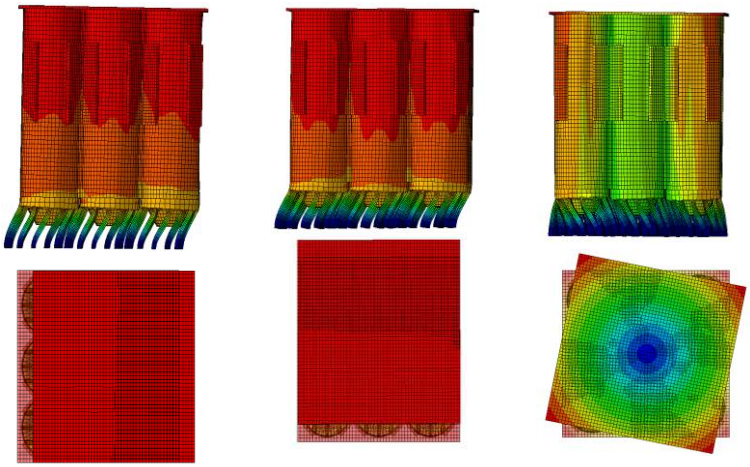		
First order frequency	16.32Hz	11.36Hz	8.96Hz
Single silo mode shapes	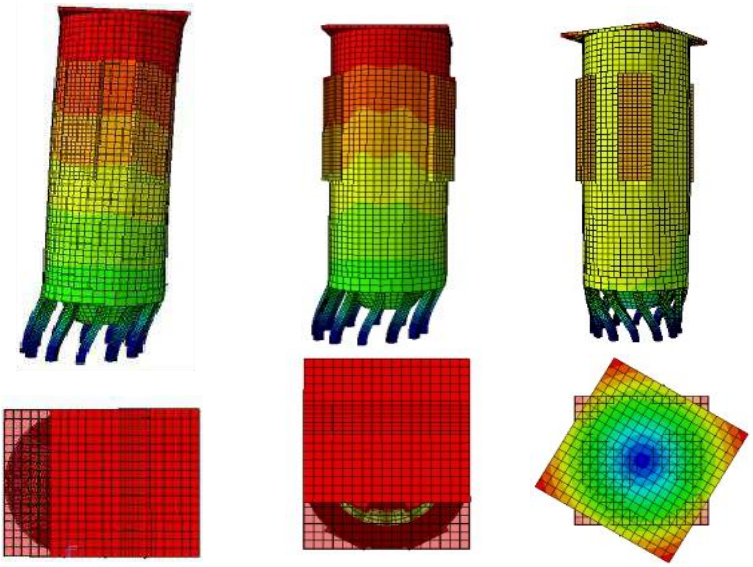		
First order frequency	14.42Hz	10.00 Hz	7.58Hz

From Tab. 3, the preceding three mode shapes and the frequency of group silos structure and single silo with empty, half, and full conditions can be obtained by the FEM method. As expected, the frequency values gradually decreased with the increasing particle mass. At this point, the rules are applicable for group silos and single silo. In addition, the overall stiffness distribution of column-supported group silos can be described as “up rigid and down soft”, particular in the supporting column system. This work will inspire structural designers: Taking reinforcement measures are necessary for the design of supporting column system.

5. Analysis and Validation

According to the simplified method of this paper, an elastic dynamic analysis model of the 3-degree freedom system was established to calculate the base shear of CSCGSS in the case of empty, half, and full granular storage conditions. Considering the stiffness of the upper silo is much greater than that of the lower column-supported, the top and bottom of the column-supported are equivalent to the fixed boundary constraint. The mechanical model of group silos can be simplified in Fig. 4.

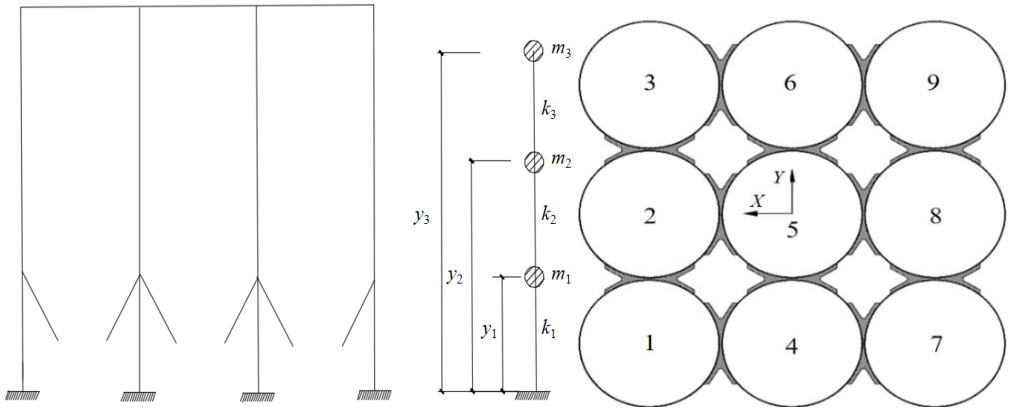

Fig. 4 Three-particle calculation model of CSCGSS: (a) Side view (b) Top view

According to Rajasekaran (2009), k_1, k_2 and k_3 is the lateral resistant stiffness for y_1, y_2 and y_3, respectively. They can be calculated by Eq. (8).

$$k_1 = \sum_{\text{column}} \frac{12EI_c}{h^3}, \quad k_{2,3} = \frac{3EI_o}{h^3} \tag{8}$$

where, I_c is the moment of inertia for column cross-section. $I_c = \frac{bh^3}{12}$, b=h=32mm. I_o is the moment of inertia for circular silo wall. $I_o = \frac{\pi}{64}(D^4 - d^4)$, D=500mm, d=480mm. h is the calculated height, $h_1 = y_1$, $h_2 = y_2 - y_1$, $h_3 = y_3 - y_2$.

According to the above data, the quality, height and stiffness of independent single silo and group silos can be calculated, as shown in Tab. 4 and Tab. 5.

211 **Tab. 4** Three-particle calculation parameters of the CSCGSS

Storage conditions	Points mass/kg			Points height/m			Each section stiffness/N/m		
	m_1	m_2	m_3	y_1	y_2	y_3	k_1	k_2	k_3
Empty	158.58	614.94	311.61	0.307	1.094	1.590	1.29×10^7	8.42×10^7	3.36×10^8
Half	955.26	1029.33	137.61	0.419	0.894	1.551	1.14×10^7	3.82×10^8	1.45×10^8
Full	955.26	2010.92	691.14	0.419	1.001	1.440	1.14×10^7	2.08×10^8	4.86×10^8

212 **Tab. 5** Three-particle calculation parameters of the independent single silo

Storage conditions	Points mass/kg			Points height/m			Each section stiffness/N/m		
	m_1	m_2	m_3	y_1	y_2	y_3	k_1	k_2	k_3
Empty	17.62	72.47	21.71	0.307	1.044	1.369	1.43×10^6	1.14×10^7	1.34×10^8
Half	106.48	115.01	7.56	0.419	0.878	1.421	1.26×10^6	4.71×10^7	2.84×10^7
Full	106.48	225.41	65.73	0.419	0.878	1.421	1.26×10^6	2.49×10^7	1.39×10^8

213 From the Tab. 4 and Tab. 5, the stiffness matrix and the mass matrix of the structure can be expressed as Eq.
214 (9).

215
$$[K]=\begin{bmatrix} k_1+k_2 & -k_2 & 0 \\ k_2 & k_2+k_3 & -k_3 \\ 0 & k_3 & k_3 \end{bmatrix},\ [M]=\begin{bmatrix} m_1 & 0 & 0 \\ 0 & m_2 & 0 \\ 0 & 0 & m_3 \end{bmatrix} \tag{9}$$

216 Then, the mass matrix (kg) and the stiffness matrix (N/m) of the single silo and group silos models can be
217 obtained.

218
$$[M]^{\text{Empty}}_{\text{Group silos}}=\begin{bmatrix} 158.58 & 0 & 0 \\ 0 & 619.94 & 0 \\ 0 & 0 & 311.61 \end{bmatrix},\ [M]^{\text{Half}}_{\text{Group silos}}=\begin{bmatrix} 955.26 & 0 & 0 \\ 0 & 1029.33 & 0 \\ 0 & 0 & 137.61 \end{bmatrix},\ [M]^{\text{Full}}_{\text{Group silos}}=\begin{bmatrix} 955.26 & 0 & 0 \\ 0 & 2010.92 & 0 \\ 0 & 0 & 691.14 \end{bmatrix}$$

219
$$[K]^{\text{Empty}}_{\text{Group silos}}=10^7\begin{bmatrix} 9.71 & -8.42 & 0 \\ -8.42 & 42.02 & -33.6 \\ 0 & -33.6 & 33.6 \end{bmatrix},\ [K]^{\text{Half}}_{\text{Group silos}}=10^7\begin{bmatrix} 39.34 & -38.2 & 0 \\ 38.2 & 52.7 & -14.5 \\ 0 & -14.5 & 14.5 \end{bmatrix},\ [K]^{\text{Full}}_{\text{Group silos}}=10^7\begin{bmatrix} 21.94 & -20.8 & 0 \\ -20.8 & 69.4 & -48.6 \\ 0 & -48.6 & 48.6 \end{bmatrix}$$

220
$$[M]^{\text{Empty}}_{\text{Single silo}}=\begin{bmatrix} 17.62 & 0 & 0 \\ 0 & 72.47 & 0 \\ 0 & 0 & 21.71 \end{bmatrix},\ [M]^{\text{Half}}_{\text{Single silo}}=\begin{bmatrix} 106.48 & 0 & 0 \\ 0 & 115.01 & 0 \\ 0 & 0 & 7.56 \end{bmatrix},\ [M]^{\text{Full}}_{\text{Single silo}}=\begin{bmatrix} 106.48 & 0 & 0 \\ 0 & 225.41 & 0 \\ 0 & 0 & 65.73 \end{bmatrix}$$

221
$$[K]^{\text{Empty}}_{\text{Single silo}}=10^6\begin{bmatrix} 12.83 & -11.4 & 0 \\ -11.4 & 145.4 & -134 \\ 0 & -134 & 134 \end{bmatrix},\ [K]^{\text{Half}}_{\text{Single silo}}=10^6\begin{bmatrix} 48.36 & -47.1 & 0 \\ -47.1 & 75.5 & -28.4 \\ 0 & -28.4 & 28.4 \end{bmatrix},\ [K]^{\text{Full}}_{\text{Single silo}}=10^6\begin{bmatrix} 26.16 & -24.9 & 0 \\ -24.9 & 163.9 & -139 \\ 0 & -139 & 139 \end{bmatrix}$$

5.1 Frequency

Taking the mass matrix and the stiffness matrix of the single silo and group silos obtained by the calculation into the Eq. (3), the first order frequencies of group silos and independent single silo with theoretical can be obtained, as shown in Fig. 5. To verify the validity of the results, the first order frequencies of group silos and independent single silo in the case of experimental and FEM with empty, half, and full conditions are shown in Fig. 5.

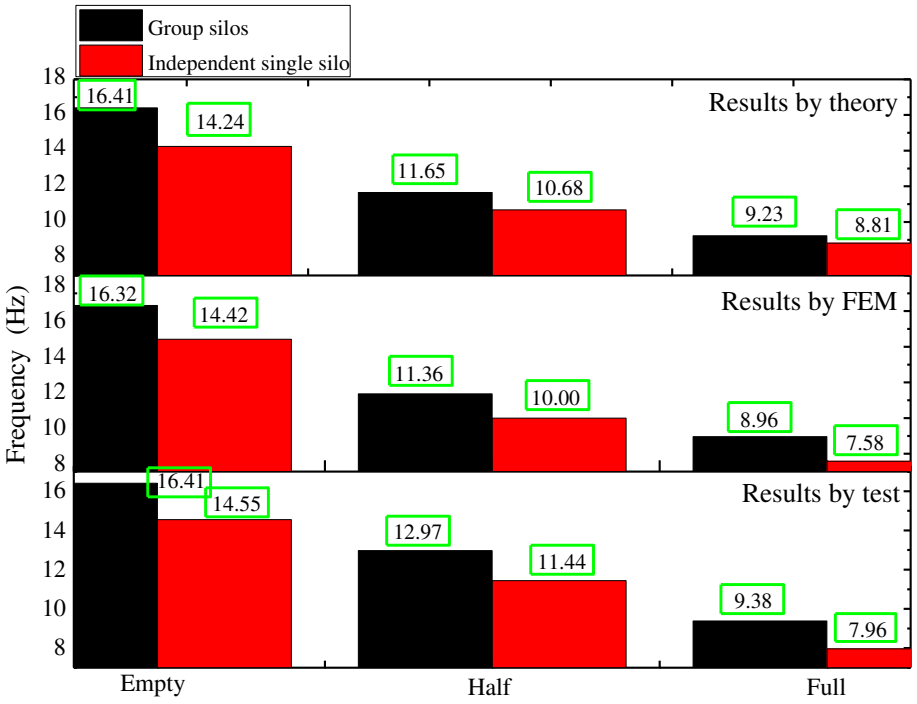

Fig. 5 The first order frequencies of group silos and single silo

From Fig. 5, a comparative analysis is done between group silos and the independent single silo the for the theoretical, test, and FEM value with empty, half, and full conditions. The rules can be obtained that the frequency of the group silos is greater than that of the independent single silo. A significant point to note is that the above rule is also applied to theoretical calculations. Therefore, it can be proved that the dynamic analysis model established in this paper is reasonable. According to the frequencies shown in Fig. 5, it can be verified that the overall stiffness of group silos structure is about 11.33% higher than that of independent single silo in case of empty, half, and full conditions. Because of this, it is unreasonable that the seismic design method for a single silo is applied to the group silos design according to Chinese code (*Standard for design of reinforced concrete silos.* (GB 50077-2017)). The current research on the seismic design method of CSCGSS is rarely involved. So, a standard that are applicable in such scenario has not been formed yet. In addition, the increase of stored particle mass is undoubtedly the main reason for the decrease of structural frequency. How to calculate the mass of the

particles involved in motion is a meaningful work, which is also the ongoing research work of the research team.

5.2 Base Shear

Considering that the height of the particle is not entirely consistent with the position of the acceleration measurement point, the acceleration value at the particle height was obtained, taking the maximum of them, by the linear interpolation of measured values by adjacent acceleration points. Hence, the inertial force can be determined by multiplying by the mass m_i of the i-th particle and the acceleration $a_i(t)$ of the corresponding height position.

With accumulated the inertial force of each particle and taking its maximum value, the base shear of the structure can be calculated in Eq. (10).

$$F = \left| \sum_{i=1}^{3} m_i a_i \right|_{\max} \quad (i=1, 2 \text{ and } 3) \tag{10}$$

For comparison, the curve of base shear in group silos with empty, half, and full conditions is plotted for three models (theoretical, experimental and FEM) in Fig. 6. Base shear is computed considering the whole group silos. It should be noted that the results from the test and FEM are presented by the average values of base shear stress under three seismic waves, including El-Centro, Tangshan and Artificial wave.

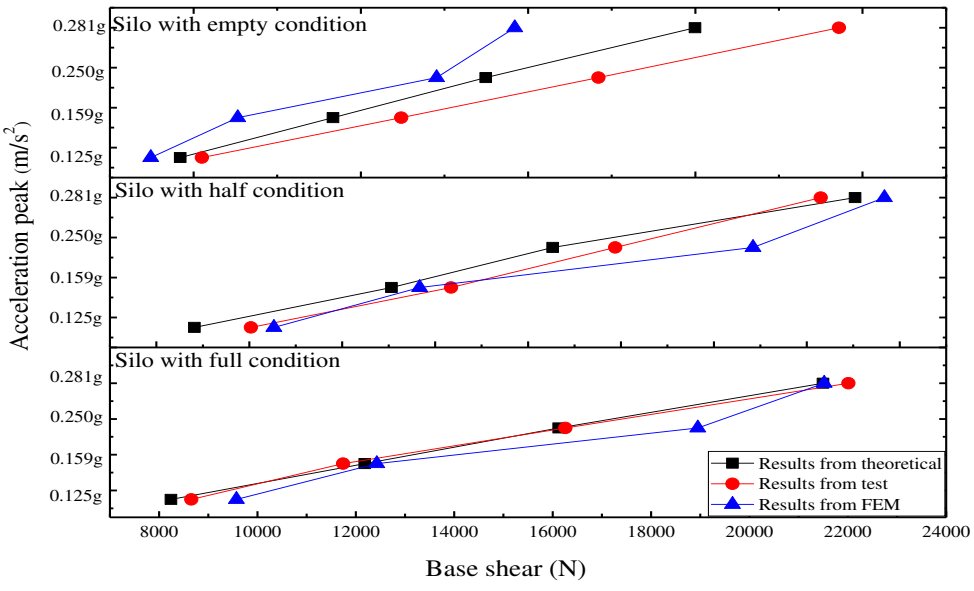

Fig. 6 The base shear in group silos with empty, half, and full conditions in the case of theoretical, test and FEM value

From Fig. 6, the shear stress curve of the group silos by theoretical is above the test value and below the finite element value curve in the case of the empty condition. The results follows a better consistency in case of

theoretical, experimental and FEM value. The base shear of the group silos gradually increases with the seismic intensity. To validate, the present work results are compared with those from an experimental scaled model and FEM in three-dimensional space in the case of the overall structure calculation model of the group silos. A detailed comparative analysis is done between group silos and the single silo for the theoretical, and test value with empty, half, and full conditions, as shown in Fig. 7.

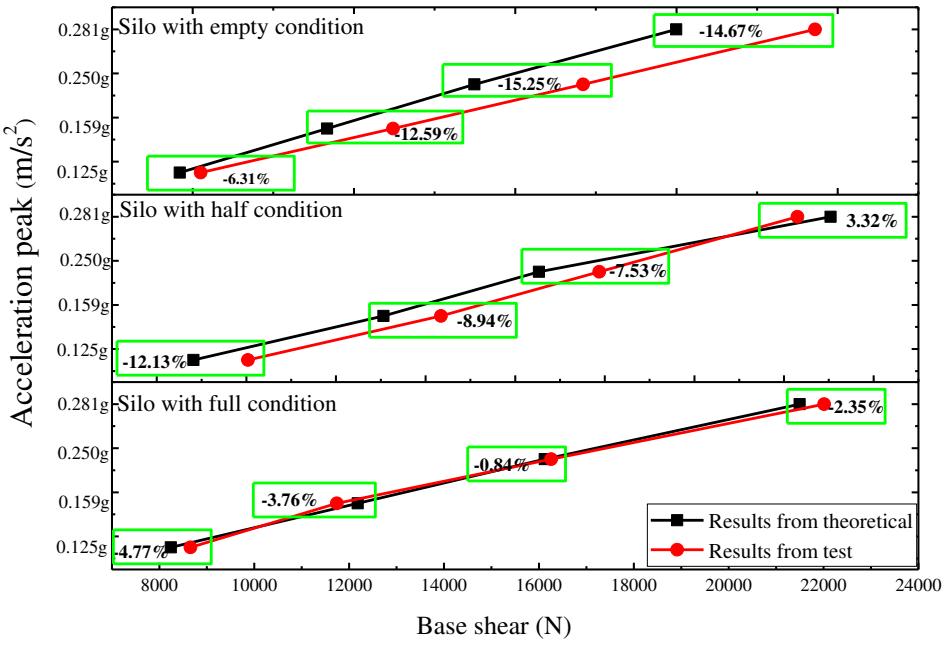

(a)

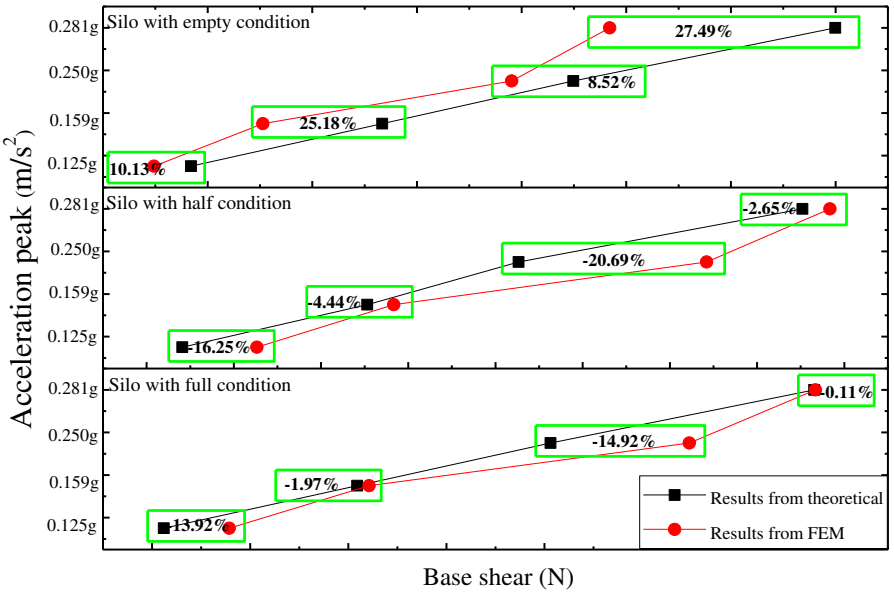

(b)

Fig. 7 The maximum base shear for group silos with empty, half, and full conditions: a) Comparative analysis theoretical and experimental value; b) Comparative analysis theoretical and FEM value.

From Fig. 7, the differences of theoretical and experimental value are shown in Fig. 7(a). The results for (**theoretical -test)/test** are shown in Fig. 7(a) green rectangular. Compared with the test values, the minimum relative error is 0.84% in the case of group silos with full condition. Again, the results for (**theoretical -FEM)/FEM** are shown in Fig. 7(b) green rectangular. Compared with the FEM values, the minimum relative error is 0.11% in the case of group silos with full condition. For both Fig. 7(a) and Fig. 7(b), with the same acceleration peak, the relative error in the full condition is lower than that of the half condition. Beyond that, the case of empty condition with a large relative error was noted in Fig. 7(a) and Fig. 7(b). This is because that simplifies simplified measures between the silo wall and the particle are considered in the overall dynamic calculation model of the group silos based on the theoretical calculation. However, for the group silos with the empty condition, the particles are not involved in the test and FEM calculations. Therefore, the dynamic calculation model considering the dynamic performance coupling effect among the silo-silo in the group silos structure proposed by this paper is reasonable, which will provide engineers with a simple and accurate tool to estimate the seismic response of group silos.

5.3 Distribution coefficient

5.31 Distribution coefficient for group silos (L_i)

For comparison, the base shear distribution coefficient is defined as the ratio of the shear of No.*i* single silo in any position for the group silos to the whole group silos, as follows.

$$L_i = \frac{F_{\mathrm{v}i}}{F_{\mathrm{vt}}} = \frac{F_{\mathrm{v}i}}{\sum_{i=1}^{n} F_{\mathrm{v}i}} \tag{11}$$

Where, L_i is the base shear stress distribution coefficient of No.*i*; $F_{\mathrm{v}i}$ is the shear of No.*i* silo in any position for the group silos; F_{vt} is the total base shear of the whole group silos; *n* is the number of silo forming the group silos structure.

According to Eq. (8), base shear distribution coefficients of No. 1, No. 2, and No. 5 silo in group silos are provided in Tab. 6, Tab. 7, and Tab. 8.

293 **Tab. 6** The base shear distribution coefficient of No.1,No.2,and No.5 silo in group silos with empty condition

Acceleration peak (m/s^2)	Seismic wave	F_{vt} (N)	F_{v1} (N)	F_{v2} (N)	F_{v5} (N)	L_1	L_2	L_5
	El-Centro	2281	258	247	259	0.113	0.108	0.114
0.125g	Tangshan	2254	245	255	253	0.109	0.113	0.112
	Artificial	1616	183	177	179	0.113	0.109	0.111
	El-Centro	3831	429	427	421	0.112	0.111	0.110
0.159g	Tangshan	3370	377	370	378	0.112	0.110	0.112
	Artificial	2526	283	278	285	0.112	0.110	0.113
	El-Centro	5014	575	543	557	0.115	0.108	0.111
0.25g	Tangshan	4526	494	509	505	0.109	0.113	0.112
	Artificial	3723	414	412	416	0.111	0.111	0.112
	El-Centro	5998	674	650	681	0.112	0.108	0.114
0.281g	Tangshan	5970	684	639	671	0.115	0.107	0.112
	Artificial	5608	644	604	620	0.115	0.108	0.110

294 **Tab. 7** The base shear distribution coefficient of No.1,No.2,and No.5 silo in group silos with half condition

Acceleration peak (m/s^2)	Seismic wave	F_{vt} (N)	F_{v1} (N)	F_{v2} (N)	F_{v5} (N)	L_1	L_2	L_5
	El-Centro	4505	498	500	509	0.110	0.111	0.113
0.125g	Tangshan	6118	685	668	693	0.112	0.109	0.113
	Artificial	4431	489	491	502	0.110	0.111	0.113
	El-Centro	8140	914	883	928	0.112	0.108	0.114
0.159g	Tangshan	7872	896	853	877	0.114	0.108	0.111
	Artificial	5500	529	668	661	0.096	0.122	0.120
	El-Centro	10017	1135	1086	1125	0.113	0.108	0.112
0.25g	Tangshan	9837	1108	1059	1133	0.113	0.108	0.115
	Artificial	6962	778	769	774	0.112	0.110	0.111
	El-Centro	12232	1357	1338	1405	0.111	0.109	0.115
0.281g	Tangshan	12427	1393	1359	1400	0.112	0.109	0.113
	Artificial	8794	984	962	993	0.112	0.109	0.113

295

296

297 **Tab. 8** The base shear distribution coefficient of No.1,No.2,and No.5 silo in group silos with full condition

Acceleration peak (m/s^2)	Seismic wave	F_{vt} (N)	F_{v1} (N)	F_{v2} (N)	F_{v5} (N)	L_1	L_2	L_5
0.125g	El-Centro	6468	721	714	723	0.112	0.110	0.112
	Tangshan	10199	1145	1115	1130	0.112	0.109	0.111
	Artificial	9293	1055	995	1065	0.114	0.107	0.115
0.15g	El-Centro	11920	1327	1321	1328	0.111	0.111	0.111
	Tangshan	12057	1352	1325	1348	0.112	0.110	0.112
	Artificial	11244	1257	1240	1252	0.112	0.110	0.111
0.25g	El-Centro	11313	1273	1229	1280	0.113	0.109	0.113
	Tangshan	20796	2335	2276	2328	0.112	0.109	0.112
	Artificial	16671	1833	1842	1911	0.110	0.110	0.115
0.281g	El-Centro	17410	1929	1926	1961	0.111	0.111	0.113
	Tangshan	25672	2854	2806	2938	0.111	0.109	0.114
	Artificial	22961	2476	2551	2695	0.108	0.111	0.117

298 The averages and variance of the base shear distribution coefficient for No. 1, 2, and 5 silo can be obtained
299 according to Tab. 6-Tab. 8, as shown in Tab. 9.

300 **Tab. 9** The averages and variance of the base shear distribution coefficient for No. 1, 2, and 5 silo.

Structure	Averages	Variance	Variance/ Averages
No. 1 silo	0.1115	0.0030	2.70%
No. 2 silo	0.1099	0.0024	2.18%
No. 5 silo	0.1129	0.0020	1.74%
Overall structure	0.1114	0.0028	2.48%

301 From Tab. 6 to Tab. 9, data differences for No. 1, 2, 5 silo, and the overall group silos were analyzed. Based
302 on the average and variance of the shear distribution coefficient, it can be found that the base shear distribution
303 coefficient is not affected by the depth of stored material, species of seismic waves and acceleration peak.
304 Significantly, the fractional error between the average shear distribution coefficient of the single silo and the
305 overall group silos is 0.04%, 1.13% and 1.29%, respectively for the No. 1, 2 and 5 silo. The results show that the
306 base shear distribution coefficient of No. 1, 2 and 5 silo is close. Therefore, it can be fully proved that the base
307 shear of each silo in the group silos is uniformly distributed for CSCGSS under earthquake action.

308 *5.32 Distribution coefficient for independent single silo (S_i)*

309 For comparison, the base shear distribution coefficient is defined as the ratio of the shear of No.*i* single silo in any
310 position for the group silos to the independent single silo, as follows.

311 $$S = \frac{\overline{F}_{\mathrm{v}}}{F_{\mathrm{vs}}} = \frac{F_{\mathrm{vg}}/n}{F_{\mathrm{vs}}} \tag{12}$$

312 Where, S is the base shear distribution coefficient; $\overline{F}_{\mathrm{v}}$ is the shear force assigned by the group silos according
313 to number of silos (n). (n is the number of single silo in group silos.) F_{vs} is the independent single silo base
314 shear. According to Eq. (12), base shear distribution coefficients S are provided in Tab. 10, Tab. 11, based on
315 FEM and test. $\overline{S}_{\mathrm{Earthquake}}$ is the average calculated by El-Centro, Tangshan and artificial waves. $\overline{S}_{\mathrm{acceleration\ peak}}$ is
316 the average calculated by different acceleration peaks.

317 Considering that the base shear of each silo in the group silos is uniformly distributed, one-ninth of the
318 maximum base shear of the overall group silos structure was regarded as the base shear of a single silo in the Tab.
319 10 and Tab. 11. To verify the rationality of the results, according to Eq. (12), calculated results of the base shear
320 ratio between a silo in group silos and independent silo by the FEM and the test were analyzed, as shown in Tab.
321 10 and Tab. 11.

322

Tab. 10 Distribution coefficient of base shear between a silo in group silos and independent silo by FEM

Storage condition	Acceleration peak	Earthquake	F_{vg}(N)	$\bar{F}_v = \frac{F_{vg}}{9}$ (N)	F_{vs} (N)	$S = \frac{\bar{F}_v}{F_{vs}}$	$\bar{S}_{\text{Earthquake}}$	$\bar{S}_{\text{acceleration peak}}$
Empty	0.125g	El-Centro	1666	185	123	1.530	1.385	1.405
		Tangshan	1805	201	173	1.136		
		Artificial	1762	196	132	1.489		
	0.159g	El-Centro	2162	240	159	1.511	1.385	
		Tangshan	2343	260	225	1.157		
		Artificial	2287	254	171	1.486		
	0.25g	El-Centro	3297	366	243	1.548	1.402	
		Tangshan	3573	397	343	1.198		
		Artificial	3488	388	261	1.460		
	0.281g	El-Centro	3744	416	275	1.578	1.448	
		Tangshan	4058	451	390	1.196		
		Artificial	3961	440	296	1.569		
Half	0.125g	El-Centro	3821	425	373	1.165	1.308	1.294
		Tangshan	7410	823	624	1.378		
		Artificial	4563	507	368	1.379		
	0.159g	El-Centro	4960	551	484	1.139	1.278	
		Tangshan	9618	1069	810	1.319		
		Artificial	5922	658	478	1.377		
	0.25g	El-Centro	7565	841	738	1.142	1.282	
		Tangshan	14669	1630	1235	1.323		
		Artificial	9032	1004	729	1.381		
	0.281g	El-Centro	8590	954	838	1.177	1.307	
		Tangshan	16658	1851	1403	1.350		
		Artificial	10257	1140	828	1.394		
Full	0.125g	El-Centro	8456	940	768	1.238	1.058	1.050
		Tangshan	12816	1424	1399	1.030		
		Artificial	7449	828	925	0.906		
	0.159g	El-Centro	10976	1220	997	1.223	1.045	
		Tangshan	16635	1848	1816	1.018		
		Artificial	9668	1074	1200	0.895		
	0.25g	El-Centro	16740	1860	1521	1.190	1.023	
		Tangshan	25371	2819	2770	1.000		
		Artificial	14745	1638	1830	0.880		
	0.281g	El-Centro	19010	2112	1727	1.226	1.072	
		Tangshan	28811	3201	3145	1.063		
		Artificial	16744	1860	2078	0.925		

Tab. 11 Distribution coefficient of base shear between a silo in group silos and independent silo by test

Storage condition	Acceleration peak	Earthquake	F_{group}(N)	$\overline{F}_v = \frac{F_{group}}{9}$ (N)	$F_{independent}$ (N)	$S = \frac{\overline{F}_v}{F_{independent}}$	$\overline{S}_{Earthquake}$	$\overline{S}_{acceleration\ peak}$
Empty	0.125g	El-Centro	2281	253	180	1.408	1.346	1.445
		Tangshan	2254	250	167	1.500		
		Artificial	1616	180	159	1.130		
	0.159g	El-Centro	3831	426	303	1.405	1.440	
		Tangshan	3370	374	229	1.635		
		Artificial	2526	281	219	1.282		
	0.25g	El-Centro	5014	557	414	1.346	1.513	
		Tangshan	4526	503	314	1.602		
		Artificial	3723	414	260	1.591		
	0.281g	El-Centro	5998	666	540	1.234	1.479	
		Tangshan	5970	663	403	1.646		
		Artificial	5608	623	400	1.558		
Half	0.125g	El-Centro	4505	501	353	1.418	1.532	1.253
		Tangshan	6118	680	416	1.634		
		Artificial	4431	492	319	1.543		
	0.159g	El-Centro	8140	904	570	1.587	1.397	
		Tangshan	7872	875	638	1.371		
		Artificial	5500	611	496	1.232		
	0.25g	El-Centro	10017	1113	937	1.188	1.136	
		Tangshan	9837	1093	920	1.188		
		Artificial	6962	774	750	1.031		
	0.281g	El-Centro	12232	1359	1383	0.983	0.947	
		Tangshan	12427	1381	1467	0.941		
		Artificial	8794	977	1064	0.918		
Full	0.125g	El-Centro	6468	719	502	1.435	1.327	1.224
		Tangshan	10199	1133	822	1.379		
		Artificial	9293	1033	884	1.168		
	0.159g	El-Centro	11920	1324	819	1.617	1.223	
		Tangshan	12057	1340	1314	1.020		
		Artificial	11244	1249	1209	1.033		
	0.25g	El-Centro	11313	1257	1098	1.145	1.177	
		Tangshan	20796	2311	1805	1.280		
		Artificial	16671	1852	1676	1.105		
	0.281g	El-Centro	17410	1934	1441	1.342	1.167	
		Tangshan	25672	2852	2509	1.137		
		Artificial	22961	2551	2498	1.021		

The base shear distribution coefficient of single silo in group silos and independent single silo with empty, half, and full condition is analyzed under the El-Centro, Tangshan and Artificial wave action, as shown in Fig. 8.

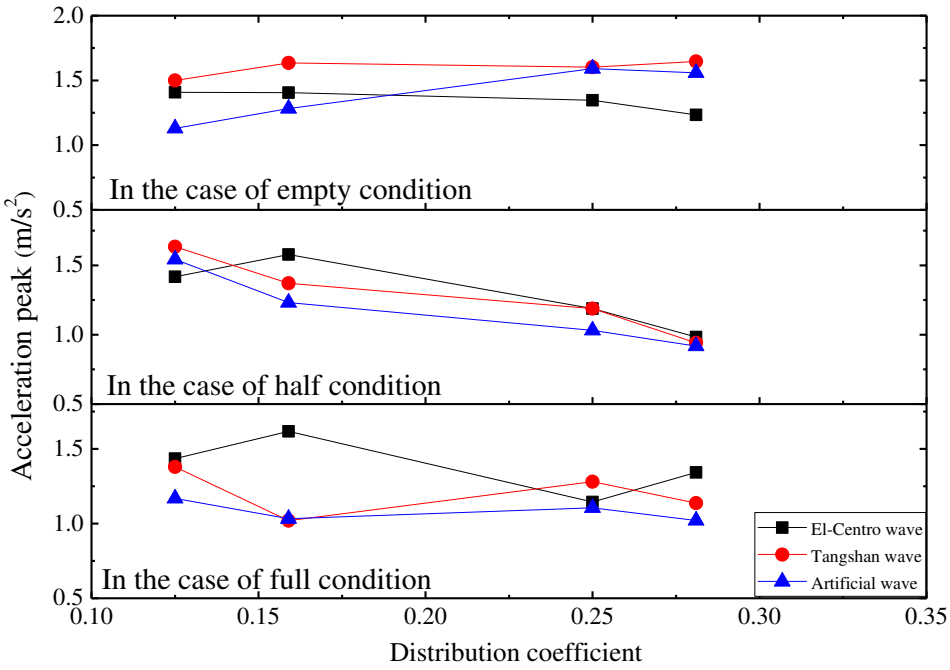

Fig. 8 The base shear distribution coefficient of single silo in group silos and independent single silo with empty, half, and full condition in case of El-Centro, Tangshan and Artificial wave

From Fig. 8, the base shear distribution coefficient of single silo in group silos and independent single silo is affected by the depth of stored material and species of seismic waves. The ratio is related to the dynamic characteristics of the structure and the input seismic wave spectrum.

Base shear distribution coefficient between a silo in group silos and independent silo was obtained in the case of empty, half, and full storage conditions by FEM, $\overline{S}_{\text{Empty}}$=1.405, $\overline{S}_{\text{Half}}$ =1.294, and $\overline{S}_{\text{Full}}$ =1.045 in Tab. 12. According to the shaking table model test, in Tab. 13, $\overline{S}_{\text{Empty}}$=1.445, $\overline{S}_{\text{Half}}$ =1.253, and $\overline{S}_{\text{Full}}$ =1.224. The relative error is within the acceptable range (2.77%, 3.72% and 9.72%) by comparing the FEM and test values. Therefore, the design model parameters are given to facilitate structural designers' simple and convenient operation procedures. For the convenience of engineering application, the base shear distribution coefficient S_{Empty}=1.5, S_{Half} =1.3, and S_{Full} =1.2 are acquired. The distribution coefficients were modulated, and the theory calculation base is provided for the subsequent engineering design of CSCGSS.

6. Simplified Calculation Method

Based on the base shear distribution coefficient proposed in this paper, a simplified calculation method is established for CSCGSS seismic calculation. For CSCGSS, a single silo in group silos can be regarded as an independent single silo, according to related dimensions. The problem of seismic action calculation is transformed into an independent single silo calculation. During the transformation process, the effect of the dynamical coupling is considered with adopted the base shear distribution coefficient. This coefficient is presented based on FEM and tests comparative analysis in the case of empty, half, and full condition.

The base shear of a single silo in the group silos can be calculated by Eq. (13).

$$\overline{F}_v = S \bullet F_{\mathrm{vs}} = S \bullet \sum_{i=1}^{m} F_i \tag{13}$$

Where S is the base shear distribution coefficient of single silo in group silos and independent single silo, according to the different storage conditions, S_{Empty}=1.5, S_{Half} =1.3, and S_{Full} =1.2. F_{vs} is the base shear of each mass point for the independent single silo structure. F_i seismic force is the base shear of each mass point for the independent single silo structure. where, F_i can be calculated by Eq. (14),

$$F_i = \alpha_1 \gamma_1 \phi_{1i} G_i \left(i = 1,2,\cdots,n\right) \tag{14}$$

Where, α_1 is the earthquake influence coefficient of the first vibration type self-vibration period; G_i is the gravity of No. i mass point, $G_i = m_i g$; γ_1 is the participation coefficient of the first-order vibration type for CSCGSS; ϕ_{1i} is relative horizontal displacement of No. i mass point first-order vibration type.

Therefore, the simplified calculation procedure for seismic action of CSCGSS is presented in Fig. 9.

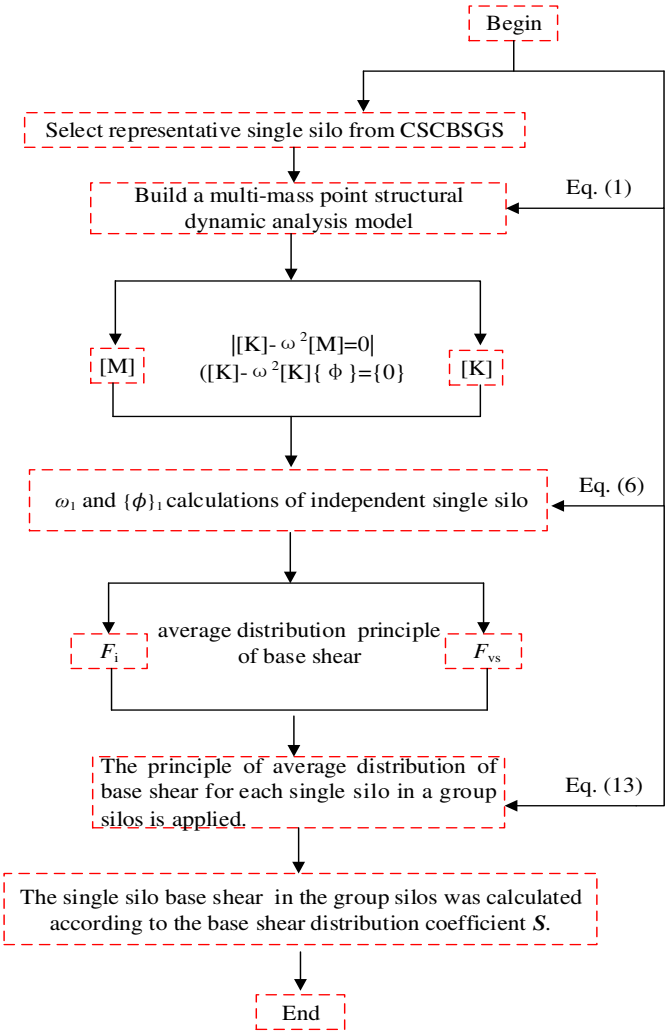

Fig. 9 Simplified calculation procedure for seismic action of CSCGSS

7. Conclusions

In this paper, a dynamic analytical model of the three-particle considering the effects of the dynamical performance coupling between different single silo in group silos was established to investigate the seismic response of the column-supported concrete group silos structure (CSCGSS) based on linear elastic theory. According to the proposed model, the base shear force of the CSCGSS was obtained. To ensure the validity of the results and perform a comparative analysis, the shaking table test and the numerical investigation were conducted. The effects of the dynamical coupling effect in group silos are verified and discussed. The main conclusions are as follows:

(1) The results of the dynamic model calculations show that the frequency values gradually decreased with the increasing particle mass. The natural frequency of vibration for the group silos and independent single one is higher than the frequency calculated by the China code. The calculation method of CSCGSS given in the existing code is too simple. It is unfavorable to the structural design of column-supported concrete group silos structure, and easy to cause the structure design to be not economical.

(2) The base shear of each silo in the group silos is uniformly distributed under earthquake action for CSCGSS, but the base shear value is not equal to the independent single one under the same conditions. To

quantify the base shear force distribution laws, the distribution coefficient S is presented and shown to be affected by the depth of stored material and species of seismic waves. For the convenience of engineering application, the coefficients were modulated and listed. After that, the coefficients can be applicable to the seismic design of CSCGSS in the case of empty, half, and full condition. S_{Empty}=1.5, S_{Half} =1.3, and S_{Full} =1.2 are acquired. The parametric design provides the basis for the subsequent engineering design of CSCGSS.

(3) The experimental phenomenon shows that the obvious bending occurs at the top of the column both for group silos and independent single silo. The more significant relative displacement is caused by the lateral deformation of the support column. The connection between the column top and silo bottom plate is vulnerable during the earthquake. Structural measures should be introduced to strengthen the structural design.

In this paper, the results obtained by the FEM and test show a good agreement. Considering the subsequent related studies, especially for the grain movement problem, PMMA was applied to the test model to meet the visualization requirements trajectory of particles. Although a similar theory of test model design is strictly followed, some errors are inevitable. Meanwhile, it should be noted that there are still a lot of works about the seismic method to study, and what the paper have done is only a tiny part of it. In the future, the effects of granular damping on the energy dissipation should be concerned. What's more, the non-linear theory and the other numerical methods such as the DEM, DIANA and CFD, will be applied to the investigation.

References

Biswal, K. C., Bhattacharyya, S.K., Sinha, P. K. (2003). Free-vibration analysis of liquid-filled tank with baffles. Journal of Sound & Vibration, 259(1), 177-192.

Abo-Elkhier, M., Muhammad, K. (2020). Failure analysis of an exploded large-capacity liquid storage tank using finite element analysis. Engineering Failure Analysis, 110: 104401.

Bayraktar, A, Sevim, B., Altunışık, A. C., et al. (2010). Effect of the model updating on the earthquake behavior of steel storage tanks. Journal of Constructional Steel Research, 66(3): 462-469.

Chowdhury, I., Singh, J, P. (2013). Dynamic Response of Rectangular Bunker Walls Considering Earthquake Force. Springer India.

Chu, X. H., Xiu, C. X., Chang, J. F. (2016). Models of hyperelasticity with softening and simulation of strain localization for brittle granular materials. Journal of Northeastern University (Natural Science), 37 (05): 731-735.

Chen, Z., Li, X., Yang, Y., et al. (2018). Experimental and numerical investigation of the effect of temperature patterns on behavior of large scale silo. Engineering Failure Analysis, 91: 543-553.

Durmuş, A., Livaoglu, R. (2015). A simplified 3 DOF model of A FEM model for seismic analysis of a silo containing elastic material accounting for soil–structure interaction. Soil Dynamics and Earthquake Engineering, 77: 1-14.

Djelloul, Z., Mohammed, D. (2018). Contribution to the seismic behaviour of steel silos: full finite-element analysis versus the Eurocode approach. Asian Journal of Civil Engineering, 19(7): 757-773.

Gong, Y. Q., Li, Y. J., Wang, L. M., et al. (2014). Dynamic property analysis of grouped reinforced concrete silos supported by columns. Earthquake engineering and engineering dynamics, (3):6.

Guo, K., Zhou, C., Meng, L., et al. (2016). Seismic vulnerability assessment of reinforced concrete silo considering granular material-structure interaction. The Structural Design of Tall and Special Buildings, 25(18): 1011-1030.

Gupta, A. K., Hall, W. J. (2017). Response spectrum method: in seismic analysis and design of structures. Routledge.

Gandia, R. M., Gomes, F. C., De Paula, W. C, et al. (2021). Evaluation of pressures in slender silos varying hopper angle and silo slenderness. Powder Technology, 394: 478-495.

HA, J. (1985). Versuche über Getreidedruck in Silozen, Z. VDI 39 1985 H, 35.

Hashemi, S., Kianoush, R., Khoubani, M. (2022). A mechanical model for soil-rectangular tank interaction effects under seismic loading. Soil Dynamics and Earthquake Engineering, 153: 107092.

Hasan, M., Mubarak, A., Fikri, R. (2022). Crack and strength assessment of reinforced concrete cement plant blending silo structure. Materials Today: Proceedings.

Kirtas, E., Rovithis, E., Makra, K. (2020). On the modal response of an instrumented steel water-storage tank including soil-structure interaction. Soil Dynamics and Earthquake Engineering, 135: 106198.

Li, X. S., Ding, Y. G., Xu, Q. K., et al. (2021). Shaking table test study on structural model of column-supported vertical silo[J]. Earthquake engineering and engineering dynamics, 41(01):212-218.

Liu, J., Feng, D. L. (2021). A multi-scale coupling finite element method based on the microscopic soil particle motions. Rock and Soil Mechanics, 42(04):1186-1199.

Ministry of Housing and Urban-Rural Development. Standard for design of reinforced concrete silos. GB 50077-2017, Beijing, China Planning Press.

Nielsen, J. (1998). Pressures from flowing granular solids in silos. Philosophical Transactions of the Royal Society of London. Series A: Mathematical, Physical and Engineering Sciences, 356(1747): 2667-2684.

Pieraccini, L., Palermo, M., Silvestri, S., et al. (2016). Seismic horizontal forces exerted by granular material on flat bottom silos: experimental and analytical results.

Pascot, A., Gaudel, N., Antonyuk, S., et al. (2020). Influence of mechanical vibrations on quasi-2D silo discharge of spherical particles. Chemical Engineering Science, 224: 115749.

Rajasekaran, S. (2009). Structural dynamics of earthquake engineering: theory and application using MATHEMATICA and MATLAB[M]. Elsevier.

Sezen, H., Livaoglu, R., Dogangun, A. (2008). Dynamic analysis and seismic performance evaluation of above-ground liquid-containing tanks. Engineering Structures, 30(3): 794-803.

Silvestri, S., Mansour, S., Marra, M., et al. (2022). Shaking Tab. tests of a full-scale flat-bottom manufactured steel silo filled with wheat: Main results on the fixed-base configuration. Earthquake Engineering & Structural Dynamics, 51(1): 169-190.

Xu, Q. K. (2019). Shaking table test and seismic performance of column-supported group silos. Hefei university of technology.

Zhang, L. J. (2010). Study of shaking table tests on the model of cylindrical-supporting group silos structures[D]. Henan university of technology.

Zhou, Y., Lv, X. L. (2016). Shaking Tab. model test method and technology of building structure. Version 2. Bei Jing: Science Press, 3-12.

Author Contributions

All authors listed have made a substantial, direct, and intellectual contribution to the work and approved it for publication. Collection of Data: Qiang Liu. Writing–Original Draft: Qikeng Xu, Yonggang Ding, and Jia Chen. Visualization: Qikeng Xu, Yonggang Ding, and Jia Chen. Writing–Reviewing and Editing: Qikeng Xu, Yonggang Ding, and Jia Chen. Resources: Qikeng Xu and Yonggang Ding. Supervision: Qiang Liu.

Conflict of interests

The authors declare that there is no conflict of interests regarding the publication of this paper.

Data Availability Statement

Design drawings, model parameters, initial earthquake acceleration, model calculation results that support the findings of this study are available from the corresponding author upon reasonable request.

Acknowledgments

This paper is supported by the Key Technologies R & D Program of Henan Provincial Department of Science and Technology (Grant number:212102310955), the Open Fund for the Key Laboratory of Henan Province (Grant number: 2020KF-B05) and the Research Fund for the Doctoral Program of Henan university of technology (Grant number:2020BS044).